Candidate

Alberto Guglielmo

ID: P38000261

Project: HW4

Question 1: Buoyancy Effect

1. Describe the buoyancy effect and why it is considered in underwater robotics while it is neglected in aerial robotics.

When a rigid body is submerged in a fluid under the effect of gravity, two static forces must be included in the dynamic model: the gravitational force and the buoyancy force. The latter is a hydrostatic effect, as it does not depend on the relative motion between the body and the fluid. The buoyancy force is defined as:

$$b = \rho \Delta \|\vec{g}\|$$

where:

- ρ is the fluid density,
- Δ is the volume of the body,
- $\vec{g} = [0\ 0\ 9.81]^T$ is the gravity vector.

Often, the center of mass and the center of buoyancy do not coincide, which may produce an unwanted torque. The buoyancy force acts in the center of buoyancy $\mathbf{r}_b^b \in R^3$ and can be computed:

$$f_b^b = -R_b^T \begin{bmatrix} 0 \\ 0 \\ b \end{bmatrix} = -R_b^T \begin{bmatrix} 0 \\ 0 \\ \rho\Delta \end{bmatrix}$$

The minus sign is because we consider the z-axis reference downward, as we did for the drones. In aerial robotics, the buoyancy effect is negligible because the density of air is extremely lower than that of the robot.
Adaptive controllers are well-suited for compensating restoring forces (gravity + buoyancy). The significance of these forces becomes apparent in large-scale vehicles, where even minor displacements between the center of mass and the center of buoyancy require substantial thrust to counteract.

Question 2: Statement Verification

2. Briefly justify whether the following expressions are true or false.

a. The added mass effect considers an additional load to the structure.**FALSE**

The first statement is false because the added mass effect does not represent an additional load on the structure, but rather a hydrodynamic phenomenon related to the inertia of the fluid being accelerated by the body's motion. It is not an external applied force, but rather a modification of the system's inertial properties, which is mathematically incorporated into the overall mass matrix through the term M_A.

b. The added mass effect is considered in underwater robotics since the density of the underwater robot is comparable to the density of the water.**TRUE**

The second statement is true because in underwater robotics, the robot's density is often comparable to that of the surrounding water. This similarity makes the effect of the accelerated fluid significant and necessary to account for in the system's dynamics. In contrast, for aerial or terrestrial applications where air density is negligible compared to the robot's density, the added mass effect is typically ignored. Therefore, added mass is a crucial factor in underwater systems precisely because of the comparable densities between the robot and its operating fluid environment.

c. The damping effect helps in the stability analysis.**TRUE**

The damping matrix $D_v \in R^{6\times6}$, which is positive definite, ensures energy dissipation an essential condition for asymptotic stability, as it guarantees a continuous decrease in the system's kinetic energy over time.

This dissipative behavior is especially important in stability analyses, such as those based on Lyapunov methods. Viscous forces can be decomposed into two components: drag forces, which act parallel to the relative velocity, and lift forces, which act perpendicular to it. The combined influence of these forces, as encapsulated by the damping matrix, contributes significantly to the system's overall stability.

To facilitate analysis and simulation, it is common practice to model these damping effects using constant coefficients. Such simplification facilitates both theoretical stability tests and dynamic model calculations.

d. The ocean current is usually considered as constant, and it is better to refer it with respect to the body frame. **FALSE**

The ocean current is usually considered constant, but only if it is referenced with respect to the world reference system, not to the body's reference frame. This is because the current is an external quantity independent of vehicle motion, and referring it to the world reference system simplifies the modeling of relative forces.

In underwater vehicle control systems, ocean currents are typically modeled under two key assumptions: they are constant in time and irrotational in space. These assumptions are usually formulated in the world reference frame as follows

$$\mathbf{v}_c = \begin{bmatrix} v_x \\ v_y \\ v_z \\ 0 \\ 0 \\ 0 \end{bmatrix}, \quad \dot{\mathbf{v}}_c = \begin{bmatrix} 0 \\ 0 \\ 0 \\ 0 \\ 0 \\ 0 \end{bmatrix} \tag{1}$$

The choice of reference frame significantly impacts control system design. When expressed in the body-fixed frame , the current velocity becomes:

$$\mathbf{v}_c^b(t) = R_b^T(t)\mathbf{v}_c \tag{2}$$

where $R_b^T(t)$ is a time-varying rotation matrix . This transformation introduces a time dependence that no longer makes the vector constant (in the body frame).

Question 3: Quadruped Simulation

3. Consider the Matlab files within the `quadruped_simulation.zip` file. Within this folder, the main file to run is `MAIN.m`. The code generates an animation and plots showing the robot's position, velocity, and z-component of the ground reaction forces. In this main file, there is a flag to allow video recording (`flag_movie`) that you can attach as an external reference or in the zip file you will submit.

You must:

a. Implement the quadratic function using the QP solver `qpSWIFT` located within the folder (refer to the instructions starting from line 68 in the file `MAIN.m`);

b. Modify parameters in the main file, such as the gait and desired velocity, or adjust some physical parameters in `get_params.m`, such as the friction coefficient and mass of the robot. Execute the simulation and present the plots you find most interesting: you should analyze them to see how they change with different gaits and parameters and comment on them.

Quadratic problem is designed to compute the optimal values of $\ddot{q}$ and f^*_{gr}. The problem includes constraints such as dynamic consistency, Non-sliding contact, Torque limits, Swing legs task.
In MATLAB, this optimization problem is solved using the solver `qpSWIFT`, and the matrices already provided by the script
Quadratic Optimization Problem:

$$\begin{aligned} \min_{\zeta} \quad & f(\zeta) \\ \text{subject to:} \quad & A\zeta = b, \\ & D\zeta \leq c. \end{aligned}$$

The script implements a model predictive control (MPC) scheme for the robot, handling several gait types:

- **0 - Trot:** diagonal legs move in alternation,
- **1 - Bound:** front and rear legs move in pairs,
- **2 - Pace:** lateral legs move in coordination,
- **3 - Gallop:** fast and asymmetrical gait with aerial phases; common in horses,
- **4 - Trot run:** faster version of the trot, maintaining diagonal leg coordination,
- **5 - Crawl:** slow gait with three or more legs always in contact with the ground

During the simulations, key parameters such as *desired velocity*, *friction coefficient*, and *robot mass* were individually varied. The analysis focused on the first three gaits (trot, bound, and pace), changing only one parameter at a time to study its impact on simulation behavior. The submitted `.zip` file also includes videos of the simulations, while the report presents only plots of *position*, *orientation*, *linear velocity*, and *angular velocity*. An additional script was developed to extract and analyze the data from the three summary tables. This allowed for a clearer comparison by highlighting:

- the maximum position error,
- the velocity oscillation amplitude(excluding transient behavior),
- and the maximum ground reaction force (GRF) along the z-axis, indicating the intensity of ground contact.

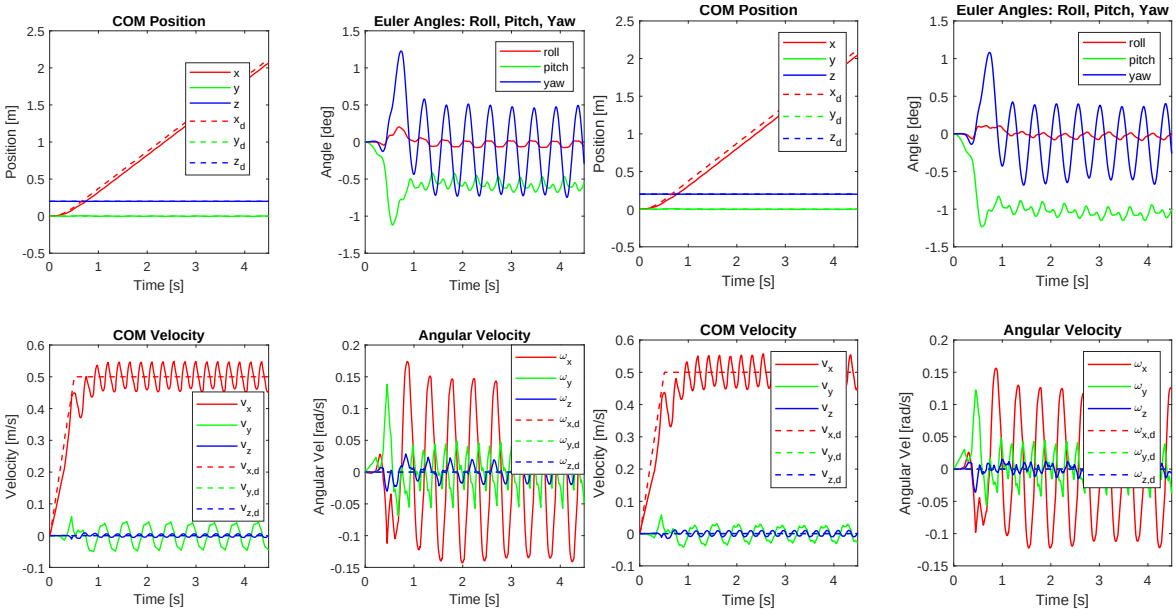

Trot $m = 5.5\,\text{kg}$ Trot $m = 10.0\,\text{kg}$

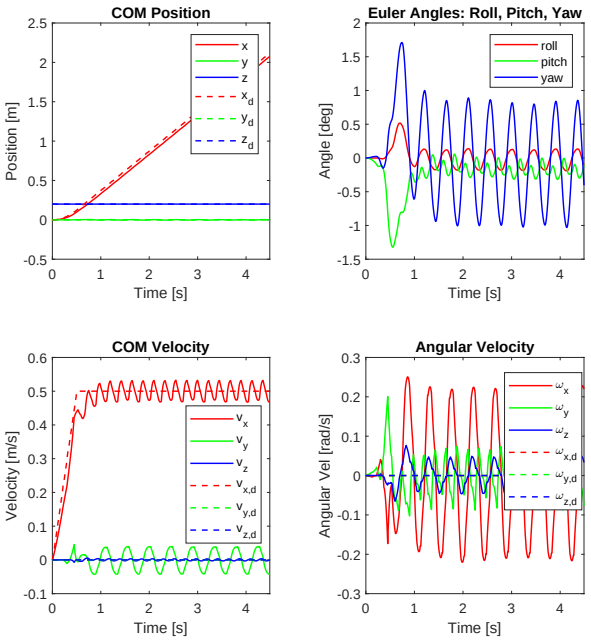

Trot $m = 2.0\,\text{kg}$

=== SIMULATION INFO ===			
Desired max speed	0.50	0.50	0.50 m/s
Robot mass	5.50	10	2.00 kg
Desired max acceleration	1.00	1.00	1.00 m/s²
Gait	0	0	0 (trot)
Max position error on x	0.05	0.07	0.05 m
=== MAXIMUM VELOCITY ERRORS ===			
Max velocity error on x	0.049	0.057	0.033 m/s
Max velocity error on y	0.047	0.033	0.042 m/s
Max velocity error on z	0.006	0.010	0.003 m/s
=== MAX ANGULAR VELOCITY ERRORS ===			
Max error ω_x	0.149	0.126	0.228 rad/s
Max error ω_y	0.057	0.044	0.088 rad/s
Max error ω_z	0.021	0.016	0.050 rad/s
=== MAXIMUM GRFs ===			
Max GRF	30.64	58.13	11.70

In the previous plots, the pose and velocity of the robot were shown while using the trot gait, where diagonal legs move in alternation. The analysis considered three different robot masses: 5.5 kg, 2 kg, and 10 kg. As expected, the ground reaction force (GRF) increased approximately linearly with the increase in mass.

It can be observed that the amplitude of the linear velocity oscillations grows with increasing mass. In contrast, angular velocities exhibit the opposite trend: the greater the mass, the smaller the oscillations in angular velocity. Despite this, the pitch angle is the only orientation component whose steady-state value is not centered around zero, and this non-zero mean increases with the mass. This behavior may be due to the inclination required by the robot to move forward: a heavier robot requires a greater pitch angle to generate sufficient forward thrust. Finally, the position error along the x-axis remains consistently below 7 cm and is only marginally affected by changes in mass.

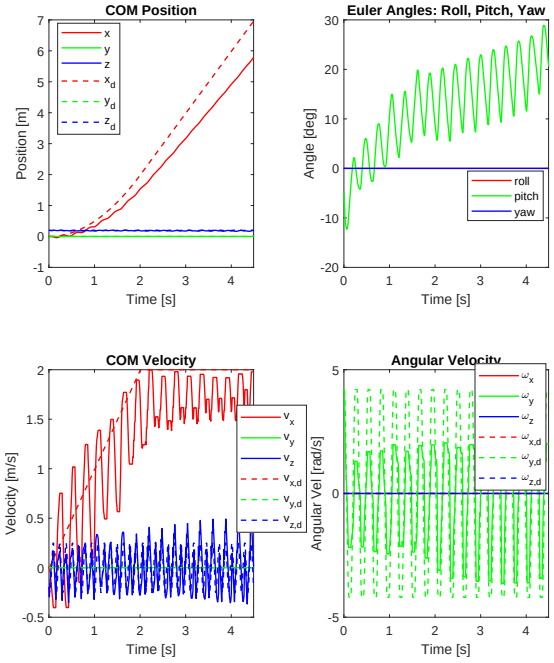

Bound $\mu = 1$

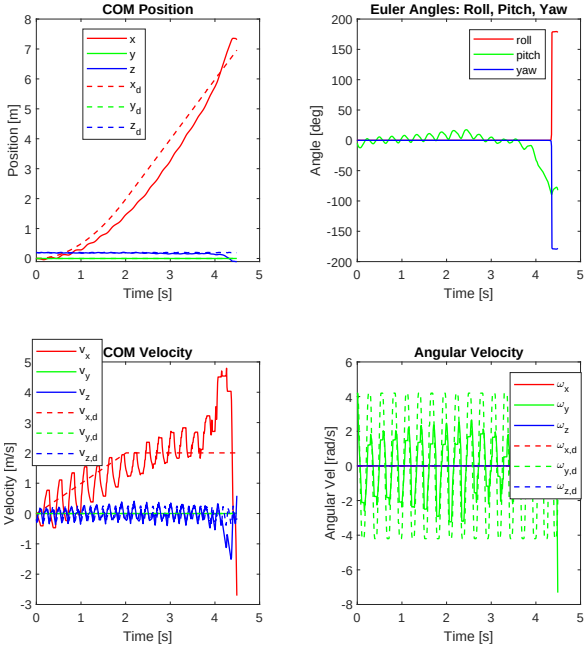

Bound $\mu = 2$

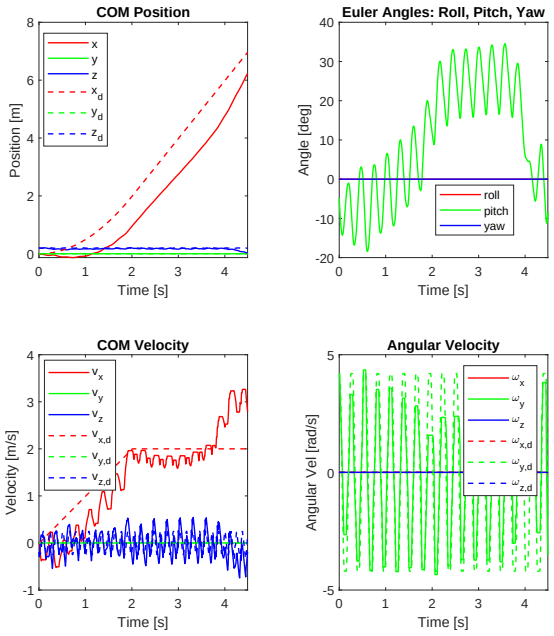

Bound $\mu = 0.5$

=== SIMULATION INFO ===			
Desired max speed	2.0	2.0	2.0 m/s
Robot mass	5.50	5.5	5.50 kg
Desired max acceleration	1.00	1.00	1.00 m/s²
Gait	1	1	1 (bound)
Max position error on x	1.18	0.75	1.35 m
μ	1.00	2.00	0.50
=== MAXIMUM VELOCITY ERRORS ===			
Max velocity error on x	0.615	4.708	1.265 m/s
Max velocity error on y	0.000	0.022	0.000 m/s
Max velocity error on z	0.467	1.220	0.535 m/s
=== MAX ANGULAR VELOCITY ERRORS ===			
Max error ω_x	0.000	0.146	0.001 rad/s
Max error ω_y	3.965	8.990	4.744 rad/s
Max error ω_z	0.000	0.037	0.001 rad/s
=== MAXIMUM GRFs ===			
Max GRF	109.83	164.21	142.44

In this case, the coefficient of friction μ was varied across the values 0.5, 1, and 2. These simulations were significantly more affected by the parameter variation. The desired maximum velocity was increased to 2 m/s for all runs, which led to considerable position errors, in some cases exceeding 1 meter. The smallest error observed was 75 cm, corresponding to the simulation with $\mu = 2$. However, this higher friction value also caused the system to become unstable, and around 4 seconds into the simulation, the robot tipped forward and fell.

It is noteworthy that this type of gait leads to pronounced pitch angle (rotation around the y-axis) variations during locomotion. This behavior is due to the quadruped moving its front legs together first, followed by the rear legs. As a result, angular velocities around the z- and x-axes remain close to zero, while the linear velocity of the center of mass along

the y-axis stays minimal.
Interestingly, the increase in friction also caused a substantial rise in ground reaction forces (GRFs) at touchdown. For the second scenario, a peak value of 164 N was recorded, which is particularly high. This surge is likely the controller's effort to maintain balance by applying greater force to regain the desired posture. In the third case, instability also began to develop after 3.5 seconds, which can be inferred from the sudden increase in linear velocity and the rapid drop in the pitch angle.
Overall, the system proved to be highly sensitive to variations in the friction coefficient.

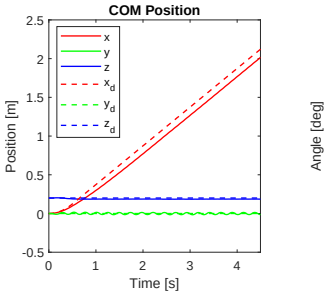

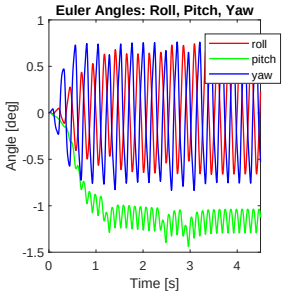

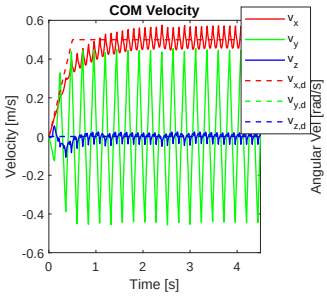

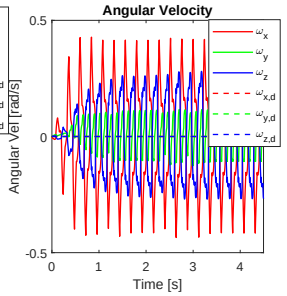

pacing $v = 0.5\,\mathrm{m/s}$

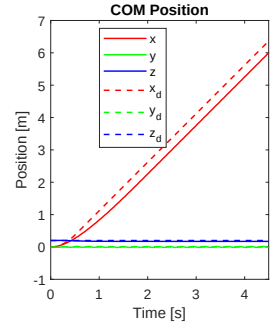

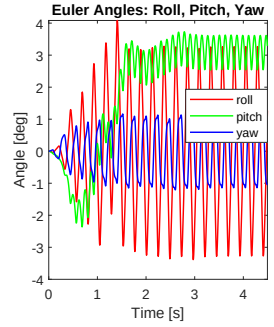

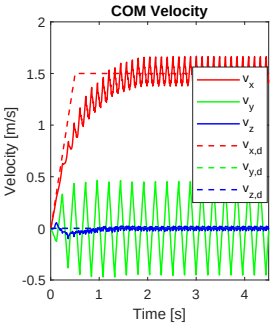

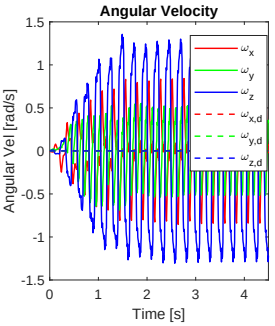

pacing $v = 1.5\,\mathrm{m/s}$

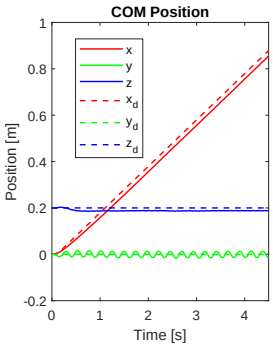

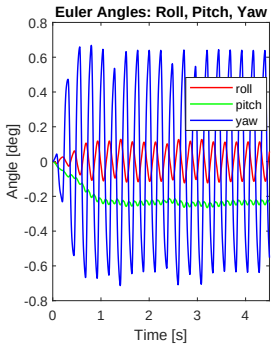

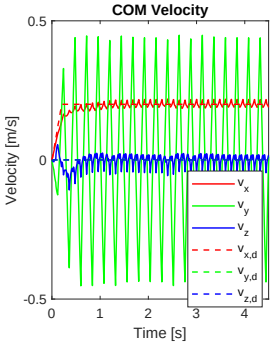

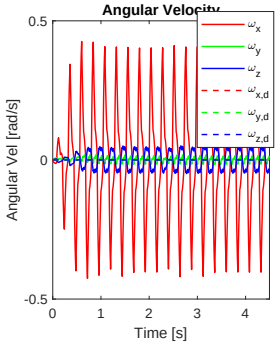

pacing $v = 0.2\,\mathrm{m/s}$

=== SIMULATION INFO ===			
Desired max speed	0.50	1.5	0.20 m/s
Robot mass	5.50	5.5	5.50 kg
Desired max acceleration	1.00	1.00	1.00 m/s²
Gait	2	2	2 (pacing)
Max position error on x	0.11	0.37	0.02 m
=== MAXIMUM VELOCITY ERRORS ===			
Max velocity error on x	0.075	0.167	0.019 m/s
Max velocity error on y	0.457	0.455	0.452 m/s
Max velocity error on z	0.051	0.032	0.057 m/s
=== MAX ANGULAR VELOCITY ERRORS ===			
Max error ω_x	0.435	0.853	0.420 rad/s
Max error ω_y	0.127	0.538	0.018 rad/s
Max error ω_z	0.280	1.305	0.051 rad/s
=== MAXIMUM GRFs ===			
Max GRF	42.21	67.20	30.64

In these simulations, the selected gait was *Pace*, in which lateral legs move in coordination. The maximum velocity was varied while keeping the maximum acceleration constant at $1\,\mathrm{m/s^2}$. A clear change in the magnitude of the position error was observed: despite a 7.5-fold increase in desired velocity, the error was reduced by a factor of 18.5 between the first and third cases.
Ground reaction forces (GRFs) also showed a strong dependence on the robot's velocity. With the robot's mass held constant, GRFs increased significantly as velocity increased. This metric must be closely monitored to ensure the robot's structural safety. Noticeable error oscillations were primarily present along the x-axis, corresponding to the direction of center of mass motion.
Angular oscillation amplitudes, on the other hand, were highly affected by the commanded forward velocity. Overall, within the range of cases analyzed, the robot demonstrated the ability to maintain stability during locomotion, at the cost of increasing position error.

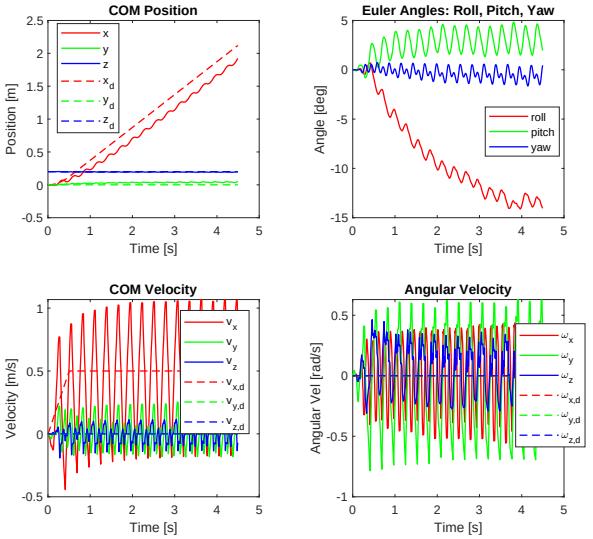

gallop

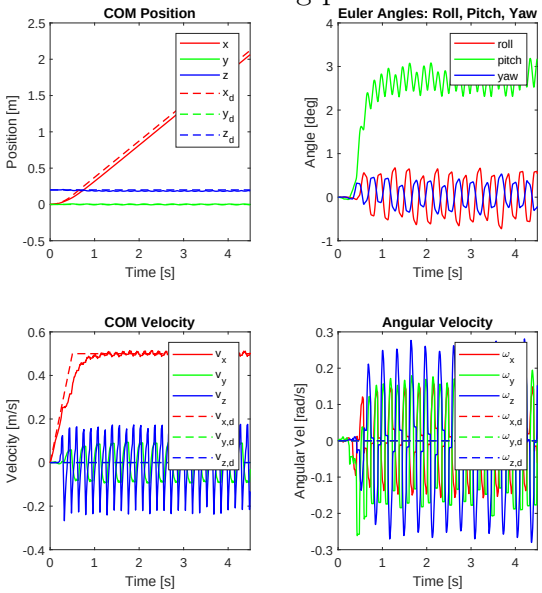

trot run

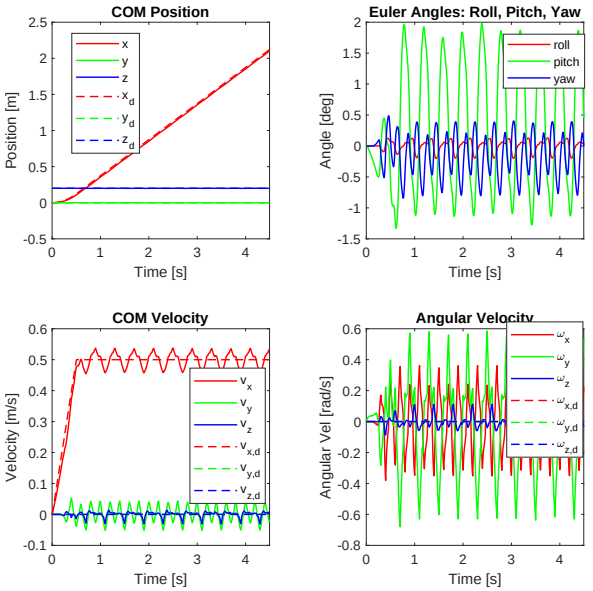

crawl

=== SIMULATION INFO ===			
Desired max speed	0.50	0.50	0.50 m/s
Robot mass	5.50	5.50	5.50 kg
Desired max acceleration	1.00	1.00	1.00 m/s²
Gait	gallop	trot run	crawl
Max position error on x	0.24	0.06	0.02 m
=== MAXIMUM VELOCITY ERRORS ===			
Max velocity error on x	0.693	0.016	0.043 m/s
Max velocity error on y	0.261	0.095	0.052 m/s
Max velocity error on z	0.137	0.237	0.031 m/s
=== MAX ANGULAR VELOCITY ERRORS ===			
Max error ω_x	0.560	0.161	0.364 rad/s
Max error ω_y	0.695	0.208	0.637 rad/s
Max error ω_z	0.361	0.281	0.113 rad/s
=== MAXIMUM GRFs ===			
Max GRF	94.36	66.07	38.01

In the last three plots, the parametric variations of the robot were not compared; instead, boundary conditions were kept constant, and only the three different gaits were analyzed: Gallop, Trot run and Crawl.
The most significant result concerns the tracking error along the x-axis, where the crawl gait proves to be the most accurate, due to its reduced oscillation amplitude. However, this accuracy is mainly due to the low desired speed of 0.5 m/s; at higher speeds, this very slow gait could result in significantly larger errors in both position and velocity.
The gait showing the highest oscillations is clearly the gallop, in which the v_x velocity varies within the range 0–1 m/s to maintain the desired average speed. This allows the robot to reach high velocities (though with strong impacts on the legs), but results in less accurate instantaneous tracking.
As for the trot run, its performance is similar to that of the standard trot but generates ground reaction forces (GRFs) up to 120% higher. This leads to a greater maximum position error and increased velocity oscillations. Even in this case, the comparison is not entirely fair, as this gait tends to show better performance at speeds higher than the 0.5 m/s used in the simulation.
It is not possible to definitively determine which gait is the best, as this heavily depends on the specific task objectives and the reference trajectory. However, among the various options, the trot gait is considered one of the most robust for quadrupedal locomotion.

Question 4: Rimless Wheel Simulation

4. Consider the MATLAB file `rimless_wheel.m`, which simulates the motion of a rimless wheel. You are required to:

a. Modify the initial angular velocity (line 12) with both positive and negative values. Run the simulation, examine the time histories of the states and the resulting phase portrait, and provide a critical discussion of the observed behavior. For example, consider the following questions: To which equilibria does the system converge? How many distinct equilibria or limit cycles are present? Can you identify their respective basins of attraction?

b. Modify the leg length (line 7), the inter-leg angle (line 8), and the slope inclination (line 9), while keeping the initial angular velocity fixed at 0.95 rad/s. Run the simulation and critically analyze the results. In particular, address questions such as: Which parameter changes affect the equilibrium conditions? Do these modifications result in different limit cycles compared to the previous case?

By modifying the initial angular velocity (with both positive and negative values), two main behaviors can be observed in the time evolution and the phase portrait:
For a sufficiently high positive initial angular velocity

$$\dot{\theta}_0 > \sqrt{\frac{2g}{l}(1-\cos(\gamma-\alpha))} = 0.9754\text{rad/s}$$

The system converges to a stable periodic solution (limit cycle), assuming the initial condition $\theta(0^+) = \gamma - \alpha$. The rimless wheel begins to walk passively and, after some transient oscillations, settles into a regular cyclic motion. This indicates the presence of a single stable attractor, namely a limit cycle.
For a positive initial velocity that is too low, the system does not possess enough kinetic energy to overcome the step. The body stops before or shortly after the first impact. In this case, no limit cycle is reached, and the final equilibrium is a static stall position.
For a negative initial angular velocity, the system typically begins to "walk backward" for a brief moment, quickly loses energy, and comes to a stop. In these cases, there is no convergence to a limit cycle, but rather to a static stable equilibrium..
However, for certain specific values of negative initial velocity, an anomalous behavior is observed: instead of stopping, the system converges to a periodic motion. This indicates that a limit cycle can still emerge, despite the initial direction of motion being opposite to the intended walking direction.
This behavior is due to the value of the angle θ at the moment when the system's velocity reaches zero. As will be shown later in the analysis of the basin of attraction, depending on the angular configuration, it is possible that even with zero initial velocities, the system may converge towards a limit cycle.

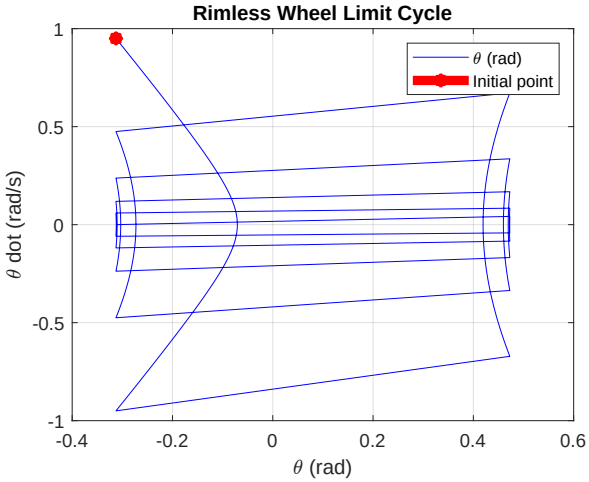

initial angular velocity $\dot{\theta}(0) = 0.95\,\text{rad/s}$

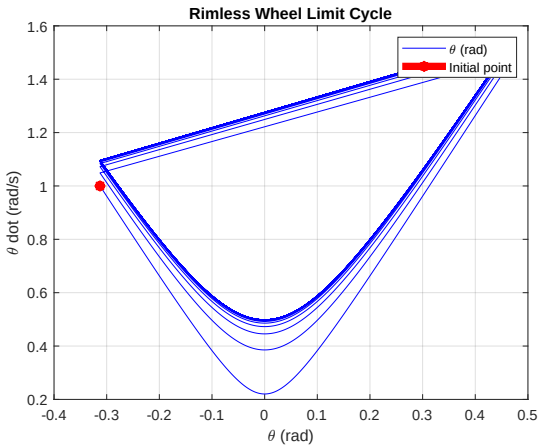

initial angular velocity $\dot{\theta}(0) = 1\,\text{rad/s}$

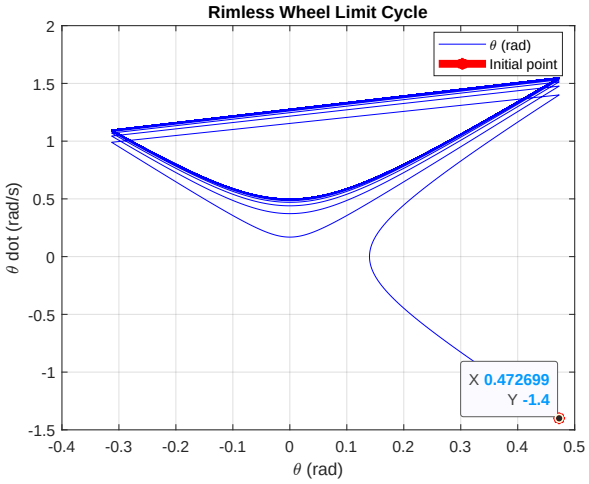

initial angular velocity $\dot{\theta}(0) = -1.4\,\text{rad/s}$

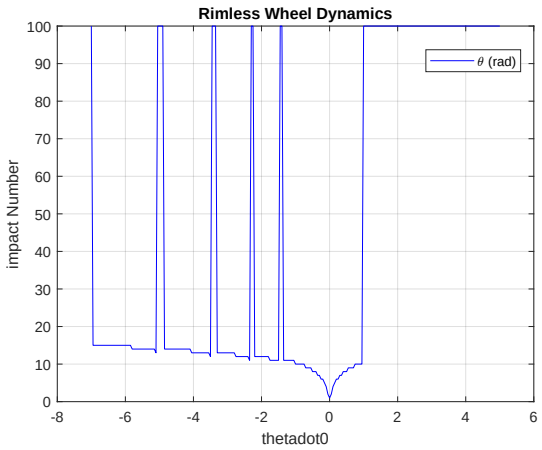

The number of contacts between the wheel and the ground varies with the initial angular velocity.

Several simulations were conducted by varying the initial angular velocity conditions. For each case, the number of foot-ground impacts was monitored and plotted in the previous figure. A value of 100 impacts indicates that the system has reached a stable limit cycle. This threshold was chosen solely for practical purposes, since , being a non-dissipative system , a true limit cycle would result in an infinite number of impacts.
Through various simulations, it was observed that the time interval between two consecutive contacts , when the rimless wheel follows the trajectory of the limit cycle if it exists, is approximately 1.0345 sec.

The equation of motion during the stance phase is given by:

$$\ddot{\theta} = \frac{g}{l} \sin\theta$$

The equilibrium point is obtained by imposing:

$$\dot{\theta} = 0 \quad \text{and} \quad \ddot{\theta} = 0$$

we relax the constraint $\theta(0^+) = \gamma - \alpha$. From $\ddot{\theta} = 0$, it follows that $\sin\theta = 0$, which implies:

$$\theta = 0 \quad \text{or} \quad \theta = \pi$$

However, $\theta = \pi$ does not represent a physically valid equilibrium in the context of the rimless wheel model, as it corresponds to a completely inverted configuration.
Therefore, the only kinematic equilibrium point is:

$$(\theta, \dot{\theta}) = (0, 0)$$

However, this point is unstable.
In the absence of a limit cycle, additional stable equilibrium points can be observed when two spokes of the rimless wheel are simultaneously in contact with the ground. Specifically, the following stable equilibrium configurations have been observed numerically:

$$(\theta, \dot{\theta}) \approx (0.4727, 0) \quad \text{and} \quad (\theta, \dot{\theta}) \approx (-0.3127, 0)$$

These conditions correspond to the wheel resting with two legs on the ground, where the system comes to a complete stop and does not evolve further.
by varying the initial condition of both position and velocity, it was possible to create the basins of attraction thanks to the appropriate matlab script.
The image is to be interpreted as follows: each pixel represents a specific initial condition of position and velocity. The color assigned to each pixel indicates the asymptotic behavior of the system, distinguishing among the fixed points $(-0.3126,\ 0)$, $(0.4726,\ 0)$, $(0,\ 0)$, and a stable limit cycle.

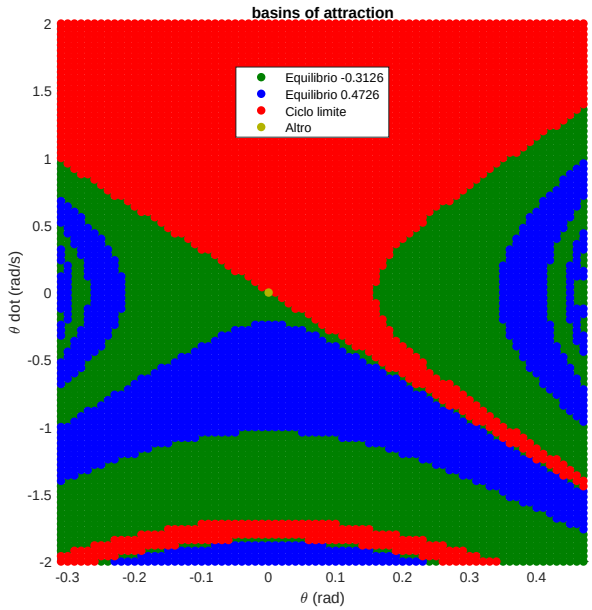

Basins of attraction

We now reintroduce the previously relaxed assumption that, given positive initial velocities, the initial position satisfies $\theta(0^+) = \gamma - \alpha$. This corresponds to initializing the system in a configuration immediately following a support transfer.
As studied analytically and confirmed numerically, the minimum positive angular velocity required to achieve a limit cycle is given by the following expression:

$$\omega_1 = \sqrt{\frac{2g}{l}\left(1 - \cos(\gamma - \alpha)\right)}$$

This equation represents the positive threshold condition for the system to have enough

kinetic energy to perform a complete step and initiate passive dynamic walking. If the initial angular velocity is less than ω_1, the system does not generate sufficient energy to overcome the gravitational potential barrier and fails to converge to a limit cycle.
To explore the effect of different physical parameters, the leg length (`l`), the inter-leg angle (`alpha`), and the slope inclination (`gamma`) were varied, while the initial angular velocity was kept fixed at 0.95 rad/s

- Increasing the leg length l reduces the required threshold ω_1, facilitating the onset of passive walking.
- A larger inter-leg angle α increases the angular displacement between steps, thereby requiring a higher initial energy to sustain walking.
- A steeper slope (larger γ) decreases the potential energy barrier, making it easier for the system to reach a stable limit cycle.

Regarding the change in equilibrium points, we observe that the configurations $(\theta, \dot{\theta}) \approx (0.4727, 0)$ and $(\theta, \dot{\theta}) \approx (-0.3127, 0)$ remain essentially unchanged when varying the leg length l. These represent stable equilibria that are not affected by changes in leg length. However, the same does not hold for the parameters α and γ, as the system reaches a stable equilibrium only when both legs are simultaneously in contact with the ground. This condition is satisfied only at configurations where $\theta^* = \gamma \pm \alpha$, meaning that any change in α or γ will alter the equilibrium points of the system.

We have already seen how variations in the parameters l, α, and γ influence the existence of limit cycles and the position of the system's equilibrium points. We now investigate whether the period of the limit cycle also changes with these parameters.
The table below summarizes the observed limit cycle periods T, for various initial conditions and parameter settings.

Initial Velocity (m/s)	$\boldsymbol{l}$	$\boldsymbol{\gamma}$	$\boldsymbol{\alpha}$	**Initial Position**	$\boldsymbol{T}$ (sec)
0.95	1	0.08	$\frac{\pi}{8}$	$\gamma - \alpha$	no limit cycle
1.00	1	0.08	$\frac{\pi}{8}$	$\gamma - \alpha$	1.0345
10.00	1	0.08	$\frac{\pi}{8}$	$\gamma - \alpha$	1.0345
-1.40	1	0.08	$\frac{\pi}{8}$	$\gamma - \alpha$	1.0345
0.95	**2**	0.08	$\frac{\pi}{8}$	$\gamma - \alpha$	1.4631
0.95	**3**	0.08	$\frac{\pi}{8}$	$\gamma - \alpha$	1.7917
0.95	1	0.08	$\frac{\boldsymbol{\pi}}{\mathbf{9}}$	$\gamma - \alpha$	0.6454
0.95	1	0.08	$\frac{\boldsymbol{\pi}}{\mathbf{18}}$	$\gamma - \alpha$	0.2066
0.95	1	**0.10**	$\frac{\pi}{8}$	$\gamma - \alpha$	0.7548
0.95	1	**0.10**	$\frac{\pi}{8}$	$\gamma - \alpha$	0.4304

Table 1: Limit cycle periods for various parameter configurations.

This table shows how the parameters l, α and γ affect both the existence and the period of the limit cycles. Furthermore, these parameters also affect the shape of the limit cycle, but the corresponding graphs have been omitted for practical reasons. It can also be observed that the initial angular velocity does not affect either the period or the shape of the limit cycle.